Applied Chemical Engineering (2022) Volume 5 Issue 1
doi:10.24294/ace.v5i1.1401

ORIGINAL RESEARCH ARTICLE

Controllable fabrication of Fe_3S_4 nanocrystals and its electrocatalytic hydrogen evolution properties

Mingxia Li[1*], Ni Xiong[1], Xin Zhou[2], Weiqi Li[2]

[1] *School of Chemistry, Chemical Engineering and Materials, Heilongjiang University, Harbin 150080, China. E-mail: limingxia@hlju.edu.cn*

[2] *School of Chemistry and Chemical Engineering, Harbin Institute of Technology, Harbin 150001, China*

ABSTRACT

In order to obtain better electrocatalytic hydrogen evolution performance, Fe_3S_4 with different morphologies was synthesized by controlling the reaction conditions. During that progress, the ferric oleate as an iron source, and the sulfur powder dissolved in oleylamine as a sulfur source. Fe_3S_4 with particle morphology proved to have the best electrochemical catalytic activity after adding 40% carbon black. In dehydrogenation, the overpotential was 234 mV and the Tafel slope was 213 mV/dec at a current density of 10 mA/cm^2. Meanwhile, Fe_3S_4 with a particle morphology exhibited superior electrochemical stability. Therefore, the controllably fabricated Fe_3S_4 with a particle morphology is a promising electrocatalyst for dehydrogenation.

Keywords: Nanocrystals; Electrocatalytic Dehydrogenation Properties; Controllable Fabrication MgO

ARTICLE INFO

Received: 22 October 2021
Accepted: 27 December 2021
Available online: 6 January 2022

1. Introduction

Electrochemical water splitting to produce hydrogen is a stable and efficient hydrogen-production method, which opens up a new path to solve the world energy problems and global environmental problems[1,2]. At present, the most efficient electrocatalyst for hydrogen production is precious metal platinum, but the reserves of Pt are limited and its price is expensive. It is important to find other cheap substances as efficient catalysts to replace Pt. Transition metals have large reserves on earth, low mining difficulty, and low price. Nanocrystals, transition metal semiconductor, have attracted more and more attention because of their small size, high specific surface area, good catalytic activity, controllable morphology, stability, and other advantages. Moreover, transition metal semiconductors have different valence states and rich electrons in the outer layer. Thus, they are ideal electrocatalytic active catalysts. In recent years, many transition metal-semiconductor materials, such as transition-metal sulfide[3], nitride[4,5], carbide[6], phosphide[7], have been widely concerned and studied because of their catalytic properties similar to precious metal catalysts and low price. Fe_3S_4 nanocrystals with different morphologies were synthesized by controlling the reaction conditions, using ferric oleate as an iron source, the sulfur powder dissolved in oleamine as a sulfur source. The results show that Fe_3S_4 nano crystals with Fe:S = 1:4 adding 40% carbon black have the best electrocatalytic dehydrogenation properties. When the current density reaches

10 mA/cm^2, the overpotential is 235 mV and the Tafel slope is 213 mV/dec. Besides, the sample also has excellent stability. This is because the nanocrystals fabricated under the condition of Fe:S = 1:4 have more edge positions, so more catalytic active sites can be exposed. At the same time, the introduction of carbon black improves the catalytic ability of the catalyst and makes the catalyst have excellent catalytic dehydrogenation properties[8-10].

2. Experimental method

Add 120 mmol of ferric oleate, 70 mL of n-hexane, 40 mL of ethanol, 30 mL of distilled water, and 40 mmol of $FeCl_3 \cdot 6H_2O$ into a 500 mL three-neck bottle at the same time. Insert a stirring paddle, stir vigorously for 24 hours, pour it into a separatory funnel, stand and remove the turbid liquid in the lower layer. Wash the brown solution in the upper layer with 80 ℃ distilled water many times until the liquid in the lower layer is clear and transparent. The brown liquid in the upper layer was rotated, and then it evaporated to obtain the viscous ferric oleate complex. Add 6 mmol of sulfur powder into a headspace injection bottle containing 6 mL of oleamine (OLA), place it into 80 ℃ water, and inject argon until all the sulfur powder is dissolved to form a uniform liquid, named OLA-S. Accurately weigh 1 mmol of ferric oleate complex into a 100 mL three-neck bottle, add 10 mL of 1-Octadecene and 20 mL of oleamine, and dissolve it by ultrasound. Heat the above liquid rapidly to 120 ℃, and maintain it in a vacuum for 1 h at this temperature to remove low boiling impurities in the mixed liquid. Then quickly inject 1 mL OLA-S or 4 mL OLA-S into the liquid and quickly heat it to 220 ℃. The Fe_3S_4 nanocrystals obtained at different reaction times were absorbed by syringe, and the obtained samples were washed many times with n-hexane as dispersant and ethanol as precipitant. Because there are a large number of organic ligands on the surface of Fe_3S_4 nanocrystals, which have a great impact on electrocatalytic properties, removed the ligands from the washed Fe_3S_4 nanocrystals. Mix 1 M hydrazine hydrate with 5 mg/mL Fe_3S_4 nanocrystals n-hexane dispersion at a volume ratio of 1:1, stir continuously for 12 h, and then wash the treated Fe_3S_4 nanocrystals many times to obtain ligand-free Fe_3S_4 nanocrystals.

3. Results and discussion

3.1 Structural characterization of the Fe_3S_4 nanocrystals

The morphology of Fe_3S_4 nanocrystals fabricated at different reaction times under two-iron sulfur ratios was observed by TEM (**Figure 1**). When the reaction lasted for 15 min with Fe:S = 1:4, it shows in **Figure 1(a)** that Fe_3S_4 nanocrystals have uneven size, poor dispersion, and irregular shape. When the reaction lasted for 60 min, it shows in **Figure 1(b)** that the fabricated Fe_3S_4 nanocrystals have regular morphology, uniform size, and good dispersion. The size of nanocrystals is about 50 nm, and clear lattice stripes can be seen from HRTEM (**Figure 1(c)**), indicating that the nanocrystals have good crystallinity. Meanwhile, the lattice spacing of 0.17 nm corresponds to the (440) crystal surface of the Fe_3S_4. When the reaction lasted for 120 min, no small particles were observed, but slices appeared, and the degree of uniformity and dispersion decreased (**Figure 1(d)**). When Fe:S = 1:1, for the sample taken at 30 min (**Figure 2(a)**), it can be observed that the generated Fe_3S_4 nanocrystals are large slices of about 100 nm arranged by many small slices. When the reaction lasted for 60 min (**Figure 2(b)**), the synthesized nanocrystals still maintained the slice shape, but the size of the slice increased by more than 100 nm. When the reaction lasted for 120 min (**Figure 2(c)**), it was observed that the nanocrystals remained in slice shape and their size continued to increase, which is more than 200 nm. A small number of small slices are about 50 nm. Serious aggregation occurred in both sizes of slices. Therefore, whether Fe:S is 1:4 or 1:1, the nanocrystals have the best morphology when the reaction lasts for 60 min.

When Fe:S = 1:4, a wafer with a size of about 50 nm was fabricated at 60 min. When Fe:S = 1:1, a wafer with a size greater than 100 nm was obtained in 60 min. In order to further analyze these two different morphologies of Fe_3S_4 nanocrystals, the following characterization is nanocrystals fabricated under the above two conditions.

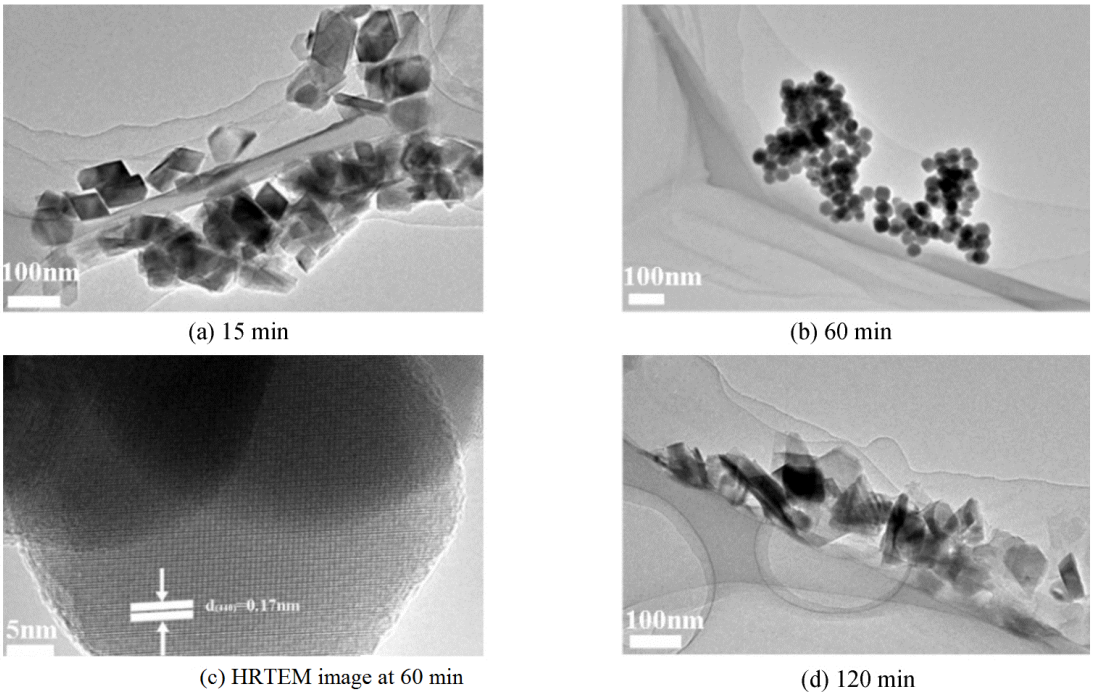

(a) 15 min (b) 60 min

(c) HRTEM image at 60 min (d) 120 min

Figure 1. TEM images of Fe_3S_4 (1 : 4) nanocrystals in different reaction time.

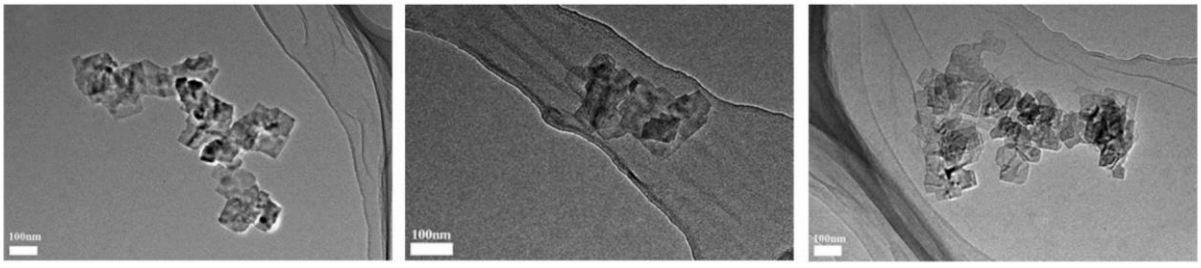

(a) 30 min (b) 60 min (c) 120 min

Figure 2. TEM images of Fe_3S_4 (1:1) nanocrystals in different reaction times.

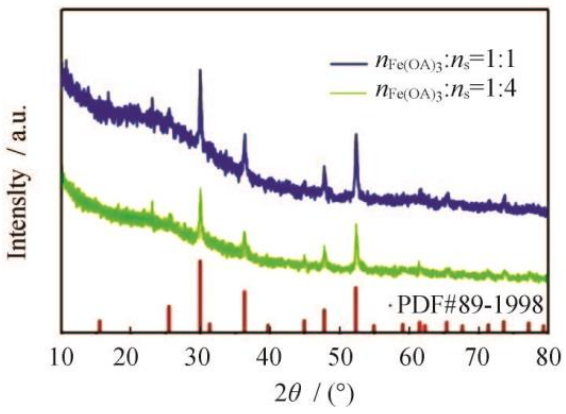

Figure 3. XRD pattern of two different types Fe_3S_4 nanocrystals.

The X-ray diffraction pattern (XRD) of Fe_3S_4 nanocrystals fabricated under Fe:S = 1:4 and Fe:S = 1:1 is shown in **Figure 3**. They have the same diffraction angle. When the diffraction angle is 29.9°, 36.3°, 47.8° and 52.3°, it corresponds to (311), (400), (511) and (440) crystal planes of cubic phase Fe_3S_4 (JCPDS Card: No. 89–1998) respectively, which shows that Fe_3S_4 fabricated in two proportions is a pure phase. Their diffraction peaks are strong, and it indicates that the fabricated samples have good crystallinity, which is consistent with the results of TEM.

In order to deeply study the composition and electronic state of Fe_3S_4 nanocrystals, the Fe_3S_4 nanocrystals fabricated under the conditions of Fe:S = 1:4 and Fe:S = 1:1 were tested by XPS. The XPS diagram of Fe_3S_4 nanocrystals at Fe:S = 1:4 is shown in **Figure 4**. **Figure 4(a)** shows the full spectrum of Fe_3S_4 nanocrystals, revealing that Fe_3S_4 nanocrystals are composed of Fe and S. The XPS diagram of S 2p shows that when binding energy located at 162.8 eV and 161.6 eV, the XPS peaks correspond to S 2p 1/2

and S 2p 3/2, indicating that S in Fe_3S_4 nanocrystals exists in the form of S^{2-}. At the same time, the XPS peak also appeared at 68.8 eV, which may attributed to the oxidation of S by oxygen in the air to form SO_4^{2-}, as shown in **Figure 4(b)**. It observed that there were no obvious peaks of Fe 2p 1/2 and Fe 2p 3/2, which may be due to the small size of the fabricated Fe_3S_4 nanocrystals, as shown in **Figure 4(c)**. The spectrum of C 1s is shown in **Figure 4(d)**.

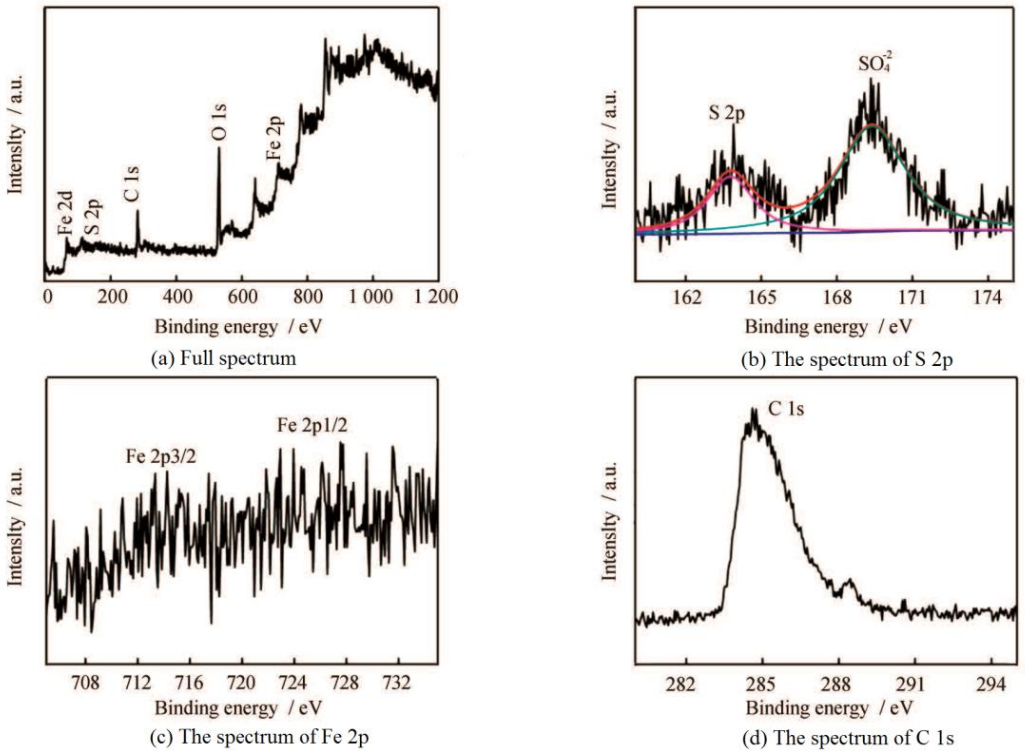

Figure 4. XPS spectra of Fe_3S_4 (1:4) nanocrystals.

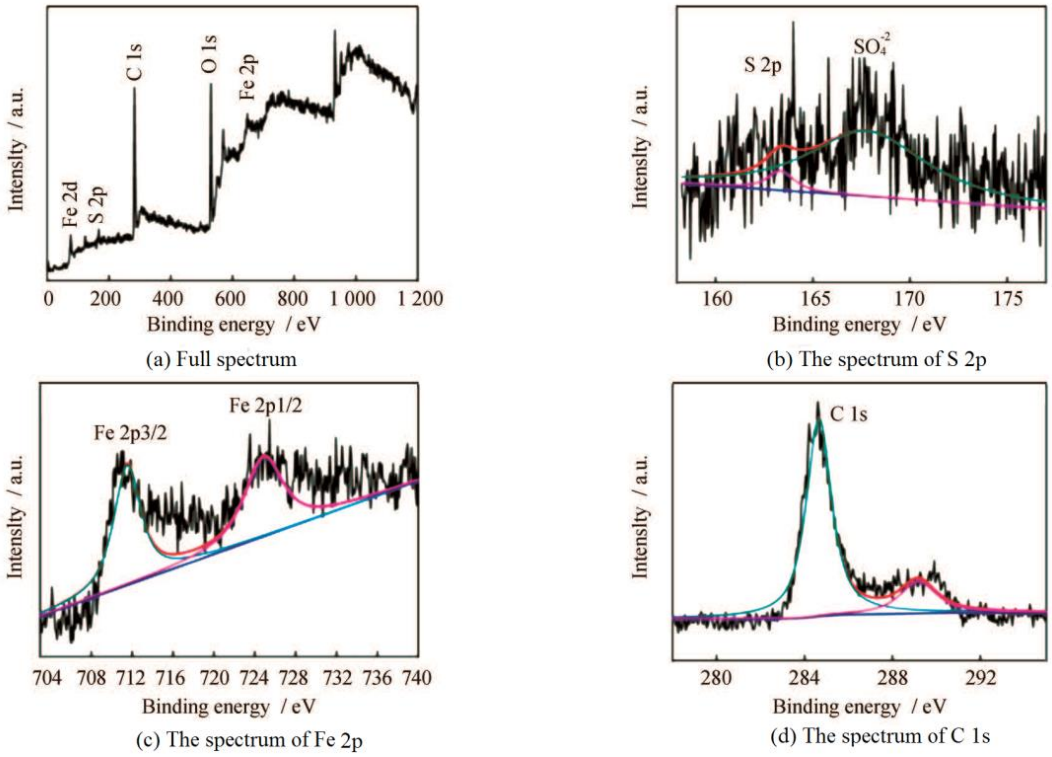

Figure 5. XPS spectra of Fe_3S_4 (1:1) nanocrystals.

The XPS spectra, full spectra, and spectra of various orbits of Fe_3S_4 nanocrystals with Fe:S = 1:1 are similar to those of Fe:S = 1:4, as shown in **Figure 5**. It is shown in **Figure 5(c)** that the XPS peak of Fe 2p is significantly enhanced, which may be caused by the increase of the size of Fe_3S_4 nanocrystals fabricated at this ratio. When the binding energies are at 723.9 eV and 710.3eV, the XPS peaks correspond to Fe 2p 1/2 and Fe 2p 3/2 respectively, indicating that the valence states of Fe are Fe^{2+} and Fe^{3+}.

There are a large number of organic ligands on the surface of nanocrystals fabricated by high-temperature thermal decomposition, which will have a great impact on the use of nanocrystals in electrocatalysis. Organic ligands hinder the electron transmission and the exposure of active sites, so it is necessary to treat the organic ligands on the surface of nanocrystals. In this paper, hydrazine hydrate is used to eliminate the ligands on the surface of nanocrystals. In order to detect whether the organic ligands on the surface of nanocrystals are eliminated, they can be detected by infrared spectroscopy. The infrared spectra of Fe_3S_4 nanocrystals fabricated in two proportions before and after treatment with hydrazine hydrate are shown in **Figure 6**. It is shown in **Figure 6** that before hydrazine hydrate treatment, the infrared spectrum of the sample shows several obvious characteristic peaks, including C-H stretching vibration peak at 2850 ~ 3000 cm^{-1}, C=C bending vibration peak at 1621 cm^{-1}, and $-CH_3$ bending vibration peak at 1436 cm^{-1}. These characteristic peaks are the characteristic peaks of oleamine molecules. It shows that there are many oleamine molecules on the surface of the sample before treatment. However, after hydrazine hydrate treatment, these characteristic peaks disappear, indicating that after hydrazine hydrate treatment, oleamine molecules on the sample surface are effectively removed, which greatly improves the electrocatalytic performance of the sample. This is mainly due to the improvement of the conductivity of the sample and the exposure of a large number of active sites.

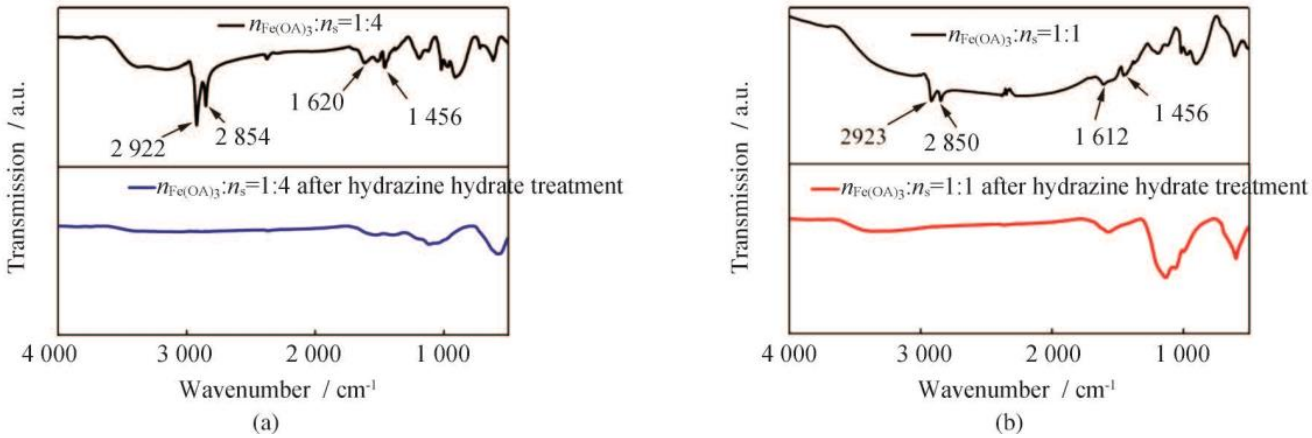

Figure 6. FTIR spectra of Fe_3S_4 nanocrystals.

3.2 Electrocatalytic dehydrogenation properties of Fe_3S_4 nanocrystals

In order to evaluate the electrocatalytic properties of treated Fe_3S_4 nanocrystals, the electrocatalytic dehydrogenation property was tested. The test adopts a three-electrode system. The first is the preparation of the working electrode: accurately weigh 5 mg of Fe_3S_4 nanocrystalline powder, add different mass fractions of carbon black. Add 1 mL of mixed liquid of ethanol and distilled water ($V_{ethanol}$:$V_{distilled\ water}$ = 1:4), and then add 20 μL naphthol, and then ultrasonic the mixed liquid to evenly disperse the nanocrystals and carbon black in the liquid. Suck 10μL of mixed liquid with a micro syringe and drop it on the glassy carbon electrode. Carbon rod for counter electrode, saturated calomel electrode for reference electrode, and 1 M KOH solution for electrolyte.

The samples fabricated at Fe:S = 1:4 were added with carbon black of different quality to explore the influence of carbon black content in the mixture on catalytic property, as shown in **Figure 7**. It is shown in **Figure 7** that when the content of carbon black accounts for 40% of the total mass, it has

the best catalytic ability. That is, when the current density is 10 mA/cm^2, the overpotential is 235 mV. This is because carbon black improves the conductivity of catalyst. In other words, it speeds up the transmission of electrons and improves the catalytic activity. If the content of carbon black is too high, the content of catalyst decreases, that is, the catalytic active site decreases. When the content of carbon black decreases, the conductive energy decreases relatively, and an appropriate amount of carbon black will improve the catalytic capacity of the catalyst.

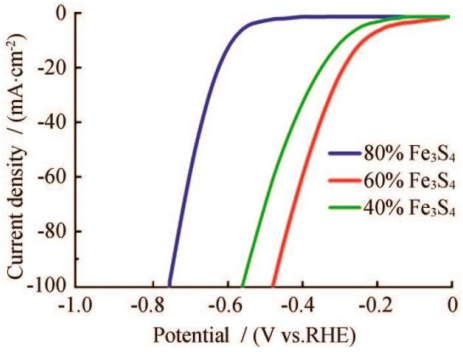

Figure 7. HER polarization curve of Fe_3S_4 nanocrystals with different contents of black carbon.

In order to explore the effect of different proportions of Fe_3S_4 nanocrystals on the catalytic performance, carbon black of the same quality (i.e. carbon black accounts for 40% of the total mass) was added to the two proportions of Fe_3S_4 nanocrystals for electrocatalytic dehydrogenation test (**Figure 8**). As can be seen from **Figure 8(a)**, when the current density is 10 mA/cm^2, the overpotential of Fe_3S_4 nanocrystals with Fe:S = 1:4 is 235 mV, while the overpotential of Fe_3S_4 nanocrystals with Fe:S = 1:1 is 268 mV, which is greater than the former. This is mainly due to the small size and large specific surface area of Fe_3S_4 nanocrystals fabricated under the condition of Fe:S = 1:4. In this way, more catalytically active sites can be exposed, thus improving the electrocatalytic ability. In order to further compare the catalytic performance of the two, the Tafel slope is fitted. As can be seen from **Figure 8(b)**, when Fe:S = 1:4, the Tafel slope of Fe_3S_4 nanocrystals is 213 mV/dec, while when Fe:S = 1:1, the Tafel slope of Fe_3S_4 nanocrystals is 267 mV/dec. This also shows that Fe_3S_4 nanocrystals fabricated under the condition of Fe:S = 1:4 have excellent electrocatalytic ability.

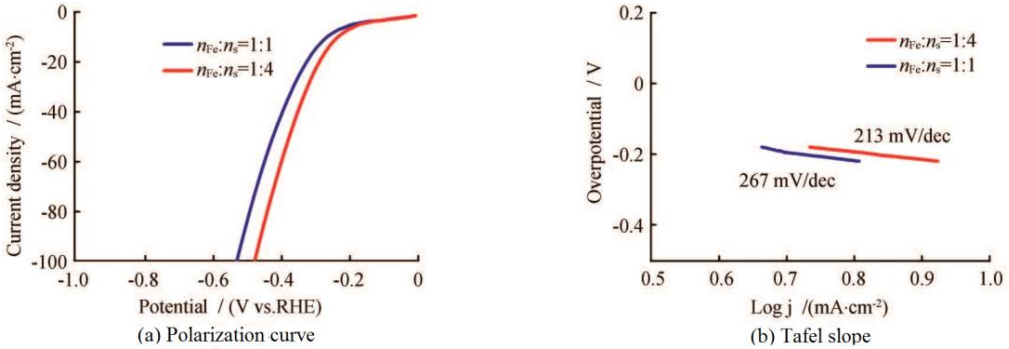

Figure 8. Properties of Fe_3S_4 nanocrystals with different morphologies（all doped with w = 40% balck carbon）.

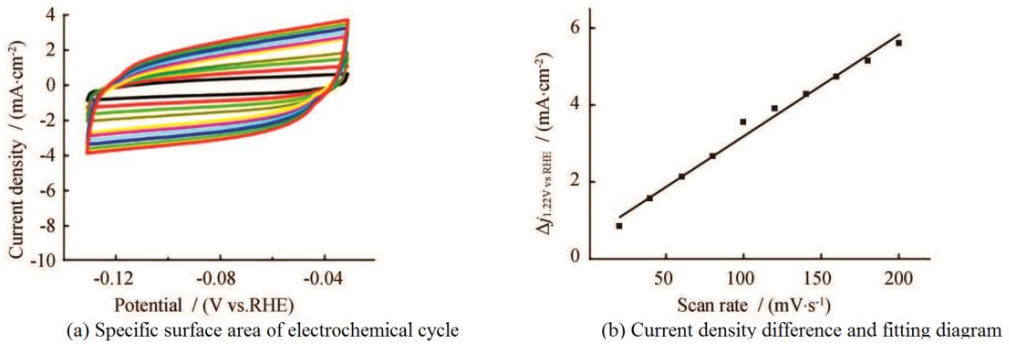

Figure 9. Particle morphology for Fe_3S_4 nanocrystals.

The capacitance test of electrocatalyst is another index to evaluate the property of hydrogen evolution catalyst. The cyclic voltammetry curves of Fe_3S_4 nanocrystals fabricated under the condition of Fe:S = 1:4 at different scanning speeds (20 ~ 200 mV/s) show in **Figure 9(a)**. Then the difference of current density corresponding to each cyclic voltammetry line is intercepted at 80 mV, and the obtained points are fitted to obtain **Figure 9(b)**. According to **Figure 9(b)**, the capacitance of the sample is calculated as 13.5 mF/cm^2, which shows that Fe_3S_4 nanocrystals fabricated under the condition of Fe:S = 1:4 have large electrochemical active area and good electron-transport ability.

Electrochemical stability is an important evaluation parameter of the electrocatalyst. The stability of Fe_3S_4 nanocrystals fabricated under the condition of Fe:S = 1:4 was tested (**Figure 10**). It shows in **Figure 10** that after 1,000 cycles of cyclic voltammetry polarization curve test, the sample is very similar to the polarization curve of the first cycle, which shows that the Fe_3S_4 nanocrystals prepared under the condition of Fe:S = 1:4 have excellent electrochemical stability.

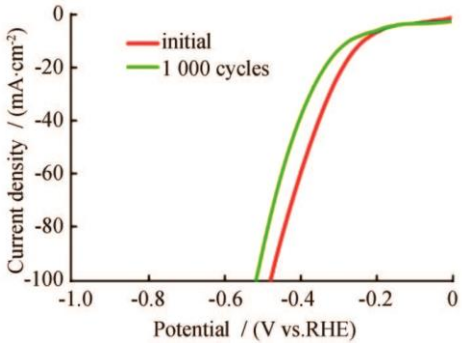

Figure 10. LSV curves of Fe_3S_4 nanocrystals with particle morphology.

4. Conclusions

In this paper, Fe_3S_4 nanocrystals with different morphologies were fabricated by high-temperature thermal decomposition method, controlling the proportion of Fe:S and using ferric oleate as the iron source and sulfur powder dissolved in oil amine as a sulfur source. When Fe:S = 1:4 and the reaction time was 60 min, circular Fe_3S_4 nanocrystals with a size of about 50 nm were fabricated. When Fe:S = 1:1 and the reaction time was 60 min, slice Fe_3S_4 nanocrystals with a size greater than 100 nm were fabricated. A series of electrochemical tests show that the Fe_3S_4 nanocrystals fabricated at Fe:S = 1:4 mixed with 40% carbon black have excellent electrocatalytic properties, that is, when the current density is 10 mA/cm^2, the overpotential is 235 mV, the Tafel slope is 213 mV/dec, and also have excellent electrochemical stability. It is because nanocrystals can expose more catalytic active sites and carbon black can improve the electron transport capacity of the catalyst. Therefore, the catalyst shows excellent electrocatalytic dehydrogenation properties.

Conflict of interest

The authors declare that they have no conflict of interest.

Acknowledgements

Funding project: General project of Heilongjiang Provincial Department of Education (12521393).

References

1. Raj IA, Vasu KI. Transition metal-based cathodes for hydrogen evolution in alkaline solution: Electrocatalysis on nickel-based ternary electrolytic codeposits. Journal of Applied Electrochemistry 1992; 22(5): 471–477.
2. Hinnemann B, Moses PG, Bonde J, *et al*. Biomimetic hydrogen evolution: MoS_2 nanoparticles as catalyst for hydrogen evolution. Journal of the American Chemical Society 2005; 127(15): 5308–5309.
3. Xie J, Zhang J, Li S, *et al*. Controllable disorder engineering in oxygen-incorporated MoS_2 ultrathin nanosheets for efficient hydrogen evolution. Journal of the American Chemical Society 2013; 135(47): 17881–17888.
4. Chen W, Sasaki K, Ma C, *et al*. Hydrogen-evolution catalysts based on non-noble metal nickel-molybdenum nitride nanosheets. Angewandte Chemie (International ed. in English) 2012; 51(25): 6131–6135.
5. Zhang L, Liang D, Ye C, *et al*. Preparation and electrochemical properties of $NiCo_2O_4$ @ nitride carbon composites. Journal of Engineering of Heilongjiang University 2019; 10(4): 45–49.
6. Ma L, Ting LRL, Molinari V, *et al*. Efficient hydrogen evolution reaction catalyzed by molybdenum carbide and molybdenum nitride nanocatalysts syn-

thesized via the urea glass route. Journal of Materials Chemistry A 2015; 3(16): 8361–8368.
7. Vrubel H, Hu X. Molybdenum boride and carbide catalyze hydrogen evolution in both acidic and basic solutions. Angewandte Chemie (International ed. in English) 2012; 51(51): 12703–12706.
8. Luo Y, Liu M, Chen Y, *et al*. Study on regeneration conditions and effect of iron modified nanocellulose saturated with phosphorus adsorption. Journal of Natural Science of Heilongjiang University 2019; 36(4): 436–441.
9. Xiong N. Controllable construction and electrocatalytic properties of iron-based sulfur (selenium) nanocrystals (in Chinese) [Master's thesis]. Harbin: Heilongjiang University; 2018.
10. Song W, Dong Y, Jie L, *et al*. Study on electron absorption spectroscopy of reduced graphene oxide regulated by de-localized crystal carbon. Journal of Engineering of Heilongjiang University 2019; 10(1): 45–42.